

Nanoscale

Accepted Manuscript



This is an *Accepted Manuscript*, which has been through the RSC Publishing peer review process and has been accepted for publication.

Accepted Manuscripts are published online shortly after acceptance, which is prior to technical editing, formatting and proof reading. This free service from RSC Publishing allows authors to make their results available to the community, in citable form, before publication of the edited article. This *Accepted Manuscript* will be replaced by the edited and formatted *Advance Article* as soon as this is available.

To cite this manuscript please use its permanent Digital Object Identifier (DOI®), which is identical for all formats of publication.

More information about *Accepted Manuscripts* can be found in the [Information for Authors](#).

Please note that technical editing may introduce minor changes to the text and/or graphics contained in the manuscript submitted by the author(s) which may alter content, and that the standard [Terms & Conditions](#) and the [ethical guidelines](#) that apply to the journal are still applicable. In no event shall the RSC be held responsible for any errors or omissions in these *Accepted Manuscript* manuscripts or any consequences arising from the use of any information contained in them.

Cite this: DOI: 10.1039/c0xx00000x

www.rsc.org/xxxxxx

ARTICLE TYPE

Facile synthesis of nickel network supported three-dimensional graphene gel as a lightweight and binder-free electrode for high rate performance supercapacitor application

Haifu Huang, Lianqiang Xu, Yanmei Tang, Shaolong Tang,* and Youwei Du

Received (in XXX, XXX) Xth XXXXXXXXX 20XX, Accepted Xth XXXXXXXXX 20XX
DOI: 10.1039/b000000x

Here we reported a simple strategy to prepare three-dimensional graphene gel coated on nickel foam for supercapacitor by simple ‘dipping and drying’ process. The supercapacitors based three-dimensional graphene gel (G-Gel@NF-1) exhibited high rate capability of 152 F g^{-1} at 0.36 A g^{-1} and 107 F g^{-1} at 90.9 A g^{-1} , good cycle stability with capacitance retention of 89% after 2000 cycles and low internal resistance (0.58Ω). Furthermore, a flexible electrode (G-gel@NF-2) was obtained by etching most nickel foam but maintains the conductive backbone of nickel foam, which greatly reduces the total mass of the electrode (can be reduced from 30 mg cm^{-2} to less than 5 mg cm^{-2}), and can be compressed from a thickness of 1 mm to $\sim 30 \mu\text{m}$. With the aid of conductive network composed of a few nickels, G-gel@NF-2 still have good performance in high rate capability and displays excellent flexible properties. The specific capacitance which mass density of electrode is only 5.4 mg cm^{-2} still reached $\sim 115 \text{ F g}^{-1}$. The strategy can improve the capability performance, greatly reduce the mass of the electrode, and lower the fabrication cost of supercapacitor.

1 Introduction

Supercapacitors (also known as electrochemical capacitors or ultracapacitors), exhibiting outstanding electrochemical performance such as high power density, fast charging-discharging rate and excellent cycle stability, so have been attracted more attention.¹⁻⁵ In a supercapacitor device, electrode material is most important component for determining performance of supercapacitor.^{3,6} In order to achieve the superior performance for supercapacitor, it requires electrode material to have high specific surface area and good electrical conductivity. Currently, carbon-based materials such as activated carbon⁷⁻⁹ carbon fibers,^{10,11} carbon nanotubes¹²⁻¹⁴ and graphene^{4,15-19} have become one of the most intense research focuses as active materials for supercapacitors mainly due to their high specific surface area, good electrical conductivity, chemical stability in the electrolyte and moderate cost. Among those carbon materials, graphene, a one-atom-thick two-dimensional carbon material, has been extensively investigated as the electrodes because of their superior electrical conductivity, exceptionally high surface area, and excellent mechanical flexibility.^{4,15,16,20} Although graphene possess many advantages, the graphene-based supercapacitors still have not achieved theoretical capacity as high as $\sim 550 \text{ F g}^{-1}$ due to self-aggregation and restacking of graphene sheets.^{4,21,22} Therefore, a three-dimensional (3D) architecture graphene has attracted more interests due to its advantage that would prevent self-aggregation and restacking of graphene sheets, possess high specific surface area, and allows

electrolytes to freely diffuse inside and through the network, thus resulting in good capacitive performance.²³⁻²⁷ In the past years, a good strategy has been developed to obtain 3D structure graphene by using nickel foam (NF) as a 3D substrate template which nickel foam not only has high electronic conductivity, desirable 3D open-pore structure, high specific surface area, but can be easily fabricated as a cheap commercial material and lower cost for supercapacitor applications. For example, 3D structure graphene was often fabricated by chemical vapor deposition (CVD) growth on nickel foam, showed a very high conductivity, outstanding electrical and mechanical properties.^{28,29} But high quality CVD equipment, complex procedures and high maintenance costs greatly limited its practical application on a large scale. Therefore, it would be a low-cost way using chemical reduction of GO sheets depositing into nickel foam to prepare 3D graphene architectures. Recently, a G-Gel/NF composite electrode by Shi *et al.* reported,²⁴ was prepared by immersing a piece of nickel foam in to GO solution and then chemical reduction that 3D graphene hydrogel depositing into the micropores of nickel foam, displays a high rate capability and a low internal resistance. Such a strategy that 3D graphene directly coated on the metal foam without any binder not only obtains a 3D architecture with high specific surface area, better ion freely diffusion characteristics and the low contact resistance, but also is a facile and cost-effective way. However, there are some disadvantages for this G-Gel/NF composite electrode. For example, the electrode is too weight and too thick (the typical density and thickness of nickel foam are about $\sim 35 \text{ mg cm}^{-2}$ and $\sim 1 \text{ mm}$, respectively), and cannot be applied to the flexible energy

storage device without flexible mechanical properties. But if nickel foam was completely etched, the 3D graphene gel without the support of nickel foam would exhibit a poor performance, mainly due to the presence of defects using chemical reduction of GO sheets and the higher contact resistance. Therefore, it is still challenging to develop a simple, inexpensive and scalable method to fabricate three-dimensional architecture graphene for supercapacitor.

In this work, we report a facile and industrially scalable approach to prepare 3D graphene gel by using nickel foam as a substrate. By simple 'dipping and drying' process, GO was easily deposited on a nickel foam framework and coated on nickel foam. After reduction by ascorbic acid, supercapacitors based 3D graphene gel coated nickel foam exhibited high rate capability and excellent cycling stability. Moreover, the areal specific capacitance can be easily modulated by controlling number of soaking or the concentration of GO, meeting a variety of requirements in practical applications. A flexible G-Gel electrode was obtained by etching most weight of the nickel foam. The removal of most of nickel foam does not damage the conductive backbone of nickel foam, but greatly reduces the total mass of the electrode (including the residual nickel network less than 6 mg cm⁻²). Furthermore, supercapacitor device fabricated using flexible G-Gel electrodes displays remarkable electrochemical performance and excellent flexible properties. In addition, the approach reported here is simple and readily scalable to industrial levels.

2 Experimental

Graphite oxide (GO) was prepared by a modified Hummers' method. Ni foam (110 PPI, mass density of ~30 mg cm⁻², Shanxi Lizhiyuan battery material co., LTD., China) was carefully cleaned treated with acetone to remove contaminants and hydrochloric acid to etch the surface, and then washed in sequence with deionized water and absolute ethanol.

2.1 Preparation of G-Gel@NF-1 and flexible G-Gel@NF-2 electrodes

Before experiment, cleaned nickel foam was fully wetted by deionized water. The preparation of graphene gels deposited onto nickel foam (G-gel@NF-1) mainly consists of three steps. Briefly, firstly the nickel foam sheets (with a size of 2.5 cm × 1cm × 0.1cm) were immersed into a GO dispersions (2mg ml⁻¹), followed by ultrasonication for 15 minutes and drying for several hours in air to remove the water at room temperature. Secondly, nickel foam sheet coated with GO film was dipped into GO dispersions (2 mg ml⁻¹) and soaked for 15 minutes and then drying for several hours to remove the water at room temperature. The second step was repeated for a number of times to increase the GO loading. Thirdly, the nickel foam sheet coated with GO was transferred to 20 ml of ascorbic acid aqueous solution (10 mg ml⁻¹) and maintained at 60 °C in a water bath for 5 h. They were repeatedly rinsed with deionized water and dried for use. A flexible G-Gel coated at nickel foam electrode (G-gel@NF-2) was obtained by putting G-Gel@NF-1 into 3M HCl acid at 80° C for 1 h to remove most of the nickel foam and then press into a sheet. In this process the conductive backbone of nickel foam was

not damaged and the mass density of the electrode (including the residual nickel network) is 8.4 mg cm⁻².

For comparison, the removal of nickel foam from the G-Gel@NF-1 composite film was performed by putting G-Gel@NF into 6 M HCl (6 mol L⁻¹) at 80° C for 6 h completely dissolve the nickel foam to obtain G-Gel. Then take G-Gel press into Ti foil without binder (labeled as G-gel@Ti, Ti foils were used current collectors).

The mass of rGO-gel was measured by putting G-Gel@NF-1 or G-Gel@NF-2 into 6 M HCl acid at 80° for 6 h completely dissolve the nickel foam to obtain dried G-Gel.

2.2 Electrochemical Measurement

A two-electrode cell configuration was used to measure the performance of G-Gel@NF-1 and G-gel@Ti as a supercapacitor electrode. Two identical G-Gel@NF-1 or G-gel@Ti electrodes (1.0 cm×1.0 cm each) were separated by a thick separator (NKK TF45, 40 μm). The flexible G-Gel@NF-2 supercapacitor device was assembled to measure the performances. A flexible G-Gel@NF-2 (1.0 cm×1.0 cm each) was attached on the PET membrane (thickness of ~30 μm) as both electrodes and current collectors. Two pieces of these sheets were assembled with a separator (NKK TF45, 40 μm) sandwiched in between (see Fig. 7a). All electrodes are without any binder or conduct additive.

The electrochemical performances were characterized by cyclic voltammetry, galvanostatic charge–discharge tests and electrochemical impedance spectroscopy (EIS) measurements in a 5 mol L⁻¹ KOH aqueous solution. The gravimetric specific capacitance was obtained from the discharge process according to the following equation: $C_s = 4 I / (m dV/dt)$, where I is the applied current (A), m is the total graphene mass of the two electrodes (g), and dV/dt is the slope of the discharge curve(V/s).

2.3 Material Characterization

The morphology of rGO-gel was examined using scanning electron microscope (SEM, Hi-tachi S3400, Japan). XRD patterns were performed on X-ray diffraction (Bruker D8, Bruker, Germany) with Cu–Kα radiation in the range of 5°–40°. XPS was carried out using Phi 5000 VersaProbe Scanning ESCA Microprobe (Ulvac-Phi, Inc., Japan). Electrochemical performance measurements were carried out at room temperature using an electrochemical workstation (CHI 660D, Chenhua Instruments, China).

3 Results and discussion

3.1. Morphological and Structural Characterization

With the aid of simple ultrasonication, wetted nickel foam induce GO hydrogel to filled rapidly into the micropores and coated network of nickel foam, and the lateral dimensions of the GO nanosheets were also reduced and produce smaller fragments.³⁰ Therefore it is easily generated for GO hydrogel to bond the skeleton of nickel foam sheet result from the decrease in the lateral dimensions of the nanosheets and van der Waals attractions. Especially, it forms a strong adhesion of GO onto the surface of nickel metal after remove the water. But if nickel foam is not full wetted and without ultrasonication, GO film covered nickel foam is not easy to generated and uneven. Therefore ultrasonication and wetted nickel foam is the key factor for GO

film growth the surface of nickel foam. Furthermore, it is easier to induce more GO hydrogel attached to the surface of network by immersing nickel foam sheet coated with GO film into GO dispersions for increase the GO loading owe to favourable interactions between GO sheets. The colours of Ni foam became dark yellow when GO gel cover foam nickel, then became dark after reduction of ascorbic acid as shown in the Fig. 1j. Compared with the bare nickel foam with a 3D cross-linked grid structure (shown in Fig. 1a), the SEM image shown in Fig. 1b clearly shows that rGO-gel has been successfully deposited in the micropores and tightly coated on the frameworks of nickel foam. The bonding of metals to graphene surfaces were divided into three types: weak physisorption, ionic chemisorption and covalent chemisorption.³¹ Given nickel foam is a bulk metal not a nano-sized metal particle, the bonding between nickel foam and graphene surfaces mainly owe to van der Waals attractions, a weak physisorption. In spite of this, rGO gels still adhere to the skeleton of nickel foam tightly, unlike GO film is easy to fall down from the metal substrate and break up during the reduction process by ascorbic acid. There is no obvious difference in the morphology of the rGO-gel coated on the frameworks of nickel foam before (Fig. 1b) and after etching by 3M HCl at 80 °C (Fig. 1c). Fig. 1d shows the morphology of the rGO-gel that nickel foam had been completely etched is similar to Fig. 1b and Fig. 1c, but without nickel foam supporter its electrochemical performance is very bad (see Fig. 6).

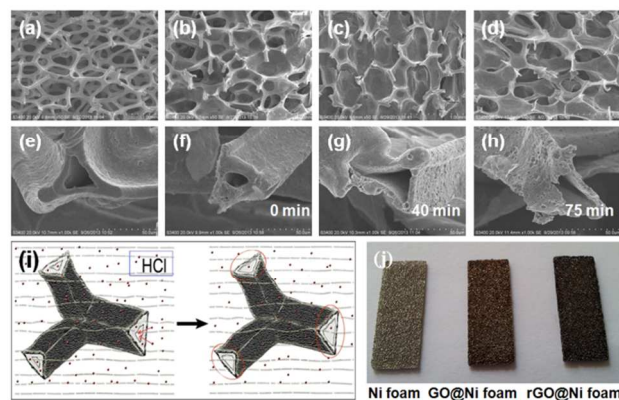


Fig.1 SEM images (a) Nickel foam, (b) As-prepared G-gel@NF-1, (c) As-prepared G-gel@NF-2, (d) rGO-gel that nickel foam had been completely etched. Cross-sectional SEM images: (e) Nickel foam, (f) As-prepared G-gel@NF-1, (g) As-prepared G-gel @NF-2 that Part of the nickel foam had been etched away in 3M HCl for 40 min, (h) As-prepared G-gel @NF-2 that Part of the nickel foam had been etched away in 3M HCl for 50 min. (i) Schematic diagram of nickel foam by etching. (j) Digital photographs of nickel foam, GO gel coated on nickel foam, and G-Gel@NF

In practical applications, the total mass of the electrode must be taken into consideration.³² The current collector such as nickel foam often makes up most of the total mass of supercapacitors. Thus, it is very necessary to reduce the total mass of the electrode via lowering the mass of the current collector but need to keep the conductive network of current collector. It is possible to achieve this goal. Nickel metal surface exposed to the hydrochloric acid solution is very easy to be corroded, but nickel metal surface covered with rGO-gel is hard to be corroded or is corroded slowly because hydrochloric acid is not easy to penetrate to the

metal surface under the protection of the graphene. From the cross-sectional SEM images of Fig. 1e, the section of nickel foam is a tubular which hydrochloric acid solution can go inside its body (demonstration diagram as shown in Fig. 1i). The inner wall of the tube is easily corroded by hydrochloric acid solution without protection, but the outer surface of the tube is corroded more slowly because of blocking effect caused by rGO-gel, thus resulting in tube wall from the inside to the outside becomes thinner, which it is confirmed by comparing cross-sectional SEM images of samples at different time of etching for 0 min, 40 min and 75 min as shown in Fig. 1f, Fig. 1g and Fig. 1h, respectively. Our results show that the conductive backbone of nickel foam can be still maintained as long as the mass density of the electrode is larger than 5 mg cm⁻² (Video1, ESI†), therefore, it is very meaningful in practical applications. Upon physical pressing, G-gel@NF-2 can be compressed from a thickness of 1 mm to ~30 μm and be free-standing without the addition of a binder.

Further, the structure and elemental characterization of rGO-gel were confirmed by XRD patterns and XPS spectra as given in Fig. 2. XRD patterns of GO and rGO-gel are shown in Fig. 2a. The featured diffraction peak of GO appeared at 10.4°, corresponding to an interlayer spacing (d-spacing) of 0.849 nm. After the chemical reduction, this peak at 2θ=10.4° is entirely disappeared but a broad diffraction peak centered at around 24°(d₀₀₂ of ~0.371nm) of the graphite (002) plane was observed for rGO-gel, indicating the few-layer stacked graphene nanosheets of their frameworks and the recovery of a graphitic crystal structure. Fig. 2b and 2c shows the C1s XPS spectra of GO and rGO-gel. From the C1s XPS spectrum of GO (Fig. 2b), there are four different peaks with different chemical valences at about 284.6, 286.4, 287.8, and 289.0 eV, corresponding to the C=C/C-C, C-O, C=O, and O=C-O species, respectively. After reduction by ascorbic acid, the oxygen species of C-O, C=O, and O=C-O reduced significantly, but the major species of C=C (284.6 eV) and C-C (285.5 eV) were remaining, as shown in Fig. 2c, which indicate that GO has been effectively reduced by ascorbic acid.

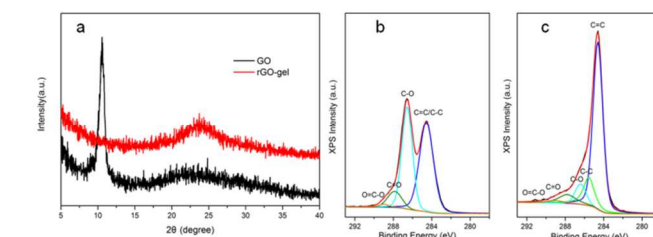


Fig.2 (a) XRD patterns of GO and rGO-gel. (b) The C 1s XPS spectra for GO and (c) The C 1s XPS spectra for rGO-gel

3.2. Electrical Measurement and Electrochemical Properties

The G-Gel@NF-1 was assembled in a symmetric two-electrode to simulate actual device behaviour. The capacitive performance was evaluated by cyclic voltammograms (CV) curves and the galvanostatic charge–discharge (GCD) tests as shown in Fig. 3. The CV curves under scan rates of 50, 100, 300 and 500 mV s⁻¹ exhibit typical quasi-rectangular shape, characteristic of the double-layer capacitor, indicating good charge propagations at the electrode interfaces following the mechanism of electric double-layer capacitors.³³ With scan rates increasing, the current response increases accordingly and the CV curves shown in Fig.

3b still keep their quasi-rectangular shape with small distortions. The CV curve of G-gel@NF-1 is still close to rectangular even at a high scan rate of 2000 mV s^{-1} , indicating a high rate capability and a low internal resistance.

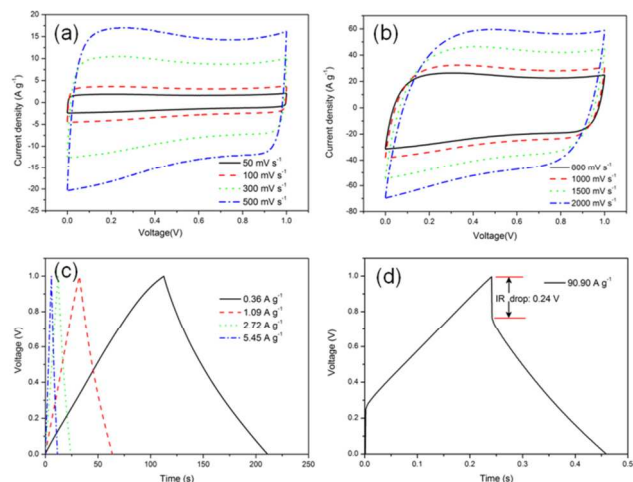


Fig.3 CV curves and GCD curves of G-gel@NF-1. (a) and (b) : CV curves at different scan rates, (c) and (d): Galvanostatic charging-discharging curves at different current densities

The galvanostatic charge–discharge (GCD) curves of the G-gel@NF-1 measured in a range of 0–1 V at different current densities are shown in Fig. 3c. The galvanostatic charge–discharge curves look nearly symmetric, which also indicating our sample have good double-layer capacitive characteristics.³³ In addition, a small voltage drop (0.24 V) was observed at the beginning of discharge (IR drop) at a high current density of 90.90 A g^{-1} (shown in Fig. 3d), also indicating a low internal resistance of the G-Gel@NF-1. The specific capacitances of the G-gel@NF-1 estimated from the discharging curves were ~ 152 , ~ 140 , ~ 133 and $\sim 129 \text{ F g}^{-1}$ at current densities of 0.36, 1.09, 2.72 and 5.45 A g^{-1} , respectively. Surprisingly, the value of specific capacitances was still up to 107 F g^{-1} at 90.9 A g^{-1} . These capacitance values are comparable to or higher than those of carbon nanotubes^{13, 34–36} and graphene film.^{15, 37, 38}

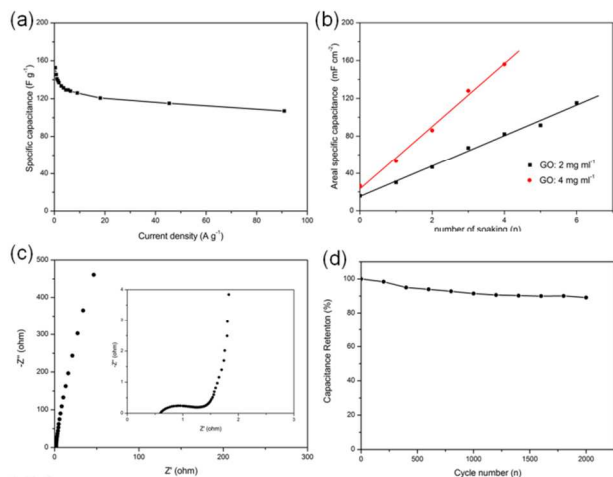


Fig.4 (a) Gravimetric specific capacitance of G-gel@NF-1 at different current densities, (b) Areal specific capacitance of G-gel@NF-1 as a function of the number of soaking with different concentrations of GO, (c) Nyquist plots of G-Gel@NF-1 and Inset: The high-frequency region

of the plots, (d) Cycle stability tests for G-gel@NF-1 at a current density of 4.62 A g^{-1} .

The gravimetric specific capacitance values derived from the discharging curves at different current densities are shown in Fig. 4a. We also clearly see that the G-gel@NF-1 maintains its $\sim 70\%$ specific capacitances with a value of 117 F g^{-1} as the current density is increased from 0.36 to 90.9 A g^{-1} , indicating high-rate performance due to the high conductivity and electrochemical stability of rGO-gel, 3D network structure of rGO-gel that facilitate the efficient access of electrolyte ions to the graphene surface and shorten the ion diffusion path^{23, 37, 39}, and low contact resistance between rGO-gel and metal current collector, which could be favourable to speed up the charge transfer at high current densities during the discharge processes.

Furthermore, the areal specific capacitance of G-Gel@NF-1 can be easily modulated by controlling number of soaking or the concentration of GO to meet a variety of requirements in practical applications. For example, when concentration of GO is 2 or 4 mg ml^{-1} and the soak time from 0 to 6, the areal specific capacitance of G-Gel@NF-1 increases from 15 to 115 mF cm^{-2} or 26 to 156 mF cm^{-2} as shown in Fig. 4b (CV curves and GCD curves see Fig. S1 and Fig. S2, ESI[†]), suggesting such regulation strategy is superior to previous methods reported by Shi *et al.*²⁴ These areal specific capacitance values are higher than those of the previously reported graphene films such as laser-scribed grapheme thin film supercapacitor (7.34 mF cm^{-2}).⁴⁰

To better understand the performance of the electrodes, the kinetic feature of the ion diffusion in this electrode is investigated using electrochemical impedance spectroscopy (EIS). Fig. 4c shows the Nyquist plot based on a frequency response analysis of frequencies ranging from 0.01 Hz to 100 kHz. The impedance curve intersects the real axis at a 45° angle in the beginning, which is the typical feature of a porous electrode when saturated with electrolyte.^{15, 41} At low frequencies, the straightline tends to be perpendicular to the real axis, indicating the pure capacitive behaviour. The high frequency region is shown in the inset of Fig. 4c. The semicircle shows good electrode contact,⁴² and an equivalent series resistance (ESR) of G-gel@NF-1 obtained from the first intersection of the semicircle with the real axis is extremely small at 0.58Ω , mainly due to the existence of 3D network structure that can facilitate the efficient access of electrolyte ions to the graphene surface and shorten the ion diffusion path. The cycle stability is an important requirement for supercapacitor applications. Therefore, the cycle stability of G-gel@NF-1 was evaluated by repeating the GCD test between 0 and 1.0 V at a current density of 4.62 A g^{-1} . As shown in Fig. 4d, the capacitance retention of the G-gel@NF-1 reaches $\sim 89\%$ after 2000 cycles, showed an excellent cycling stability.

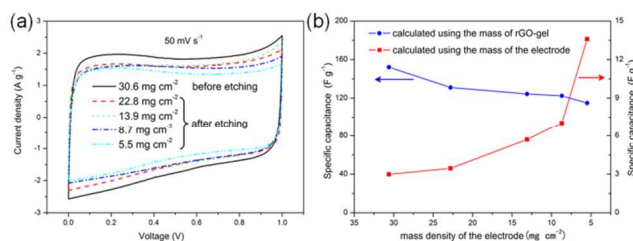


Fig.5 (a) CV curves for different mass density of electrodes. (b) Gravimetric specific capacitance of G-gel@NF-2 for different mass

density of electrodes: calculated using the mass of rGO-gel (blue) and the mass of the whole electrode (red), respectively.

G-gel@NF-1 exhibits the high rate capability and high specific capacitances, but the weight of the current collector must be taken into consideration in practical application,³² and mass density of nickel foam is too large and reaches about 30 mg cm^{-2} in our experiment. Therefore, it is very necessary to reduce the total weight of electrodes. Fig. 5a shows that there are no obvious differences for CV curves before etching and after etching except the area of CV curves decrease with reduction of the mass density of the electrode. Even the mass density of the electrode can be reduced to about 16% with a value of 5.4 mg cm^{-2} , its CV curve is still close to typical quasi-rectangular shape due to the existence of conductive backbone, suggesting that electrode can be removed most of the nickel foam and just keep the conductive backbone. The gravimetric specific capacitances calculated using mass of rGO-gel decrease with reduction of the mass density of the electrode as shown in Fig. 5b. Before etching, G-gel@NF-1 has a high specific capacitance of $\sim 152 \text{ F g}^{-1}$, but after etching by 3M HCl for more than an hour, the value of gravimetric specific capacitance still reaches $\sim 115 \text{ F g}^{-1}$ with 25% degradation, but the corresponding mass density of electrode including the mass of Ni is very low and only 5.4 mg cm^{-2} , comparing with the weight of the nickel foam (mass density of about 30 mg cm^{-2} , thickness of 1 mm). In order to better illustrate the advantage of our approach, the gravimetric capacitance calculated using the total mass of the electrode with 5.4 mg cm^{-2} is $\sim 13.5 \text{ F g}^{-1}$ and more than four times as many as that for electrode of 30.6 mg cm^{-2} with a value of $\sim 3 \text{ F g}^{-1}$ as shown in Fig. 5b, suggesting an good idea to improve the performance of supercapacitors.

In general, graphene material using chemical reduction of GO sheets often shows bad electrochemical performance in high rate capability, mainly due to the presence of defects using chemical reduction and the higher contact resistance between graphene material and current collector. For comparison, the rGO-gel attached on a Ti foil exhibits a poor performance when nickel foam was completely etched in our experiment as shown in Fig. 6. Fig. 6a shows the cyclic voltammograms (CV) of G-gel@Ti in the range from 0 to 1.0 V at different scan rates. The CV curves of G-gel@Ti under scan rates of 50 and 100 mV s^{-1} exhibit typical quasi-rectangular shapes. However, the CV curve deviated from the quasi-rectangular shape when the scan rate was up to 300 mV s^{-1} , indicating it has bad electrochemical performance in high rate capability. It also confirmed by the galvanostatic charge-discharge (GCD) curves measured in a range of 0-1V at different current densities. As shown in Fig. 6b, 6c, 6d and 6e, respectively, GCD curves look nearly symmetric, indicating our sample has good double-layer capacitive characteristics, but IR drop (about $\sim 0.17 \text{ V}$) of G-gel@Ti was observed at a current density of 3.57 A g^{-1} . The gravimetric specific capacitance at different current densities from 0.28 to 3.57 A g^{-1} are shown in Fig. 6f. The current density is increased only 3.57 A g^{-1} , but the gravimetric specific capacitance has been decreased by $\sim 20\%$ with a value of 85 F g^{-1} . In addition, the specific capacitance of G-gel@Ti is significantly less than the value of G-gel@NF-1. These results indicate rGO-gel has bad electrochemical performance in high rate capability without nickel foam supporter, mainly due to the higher contact resistance. This can be explained reasonably. Nickel foam plays

an important role in the performance of supercapacitor. The contact surface of rGO gel directly coated on nickel foam is much larger than rGO-gel attached on a Ti foil, lead to different of contact resistance between G-gel and nickel foam or Ti foil. Integration of graphene into the nickel foam as a whole electrode can effectively reduce the contact resistance. Therefore, the more content of Ni foam, the better the performance of G-gel coated on Ni foam, which has been confirmed by Fig. 5. And the conductive network composed of a few nickels is necessary for supercapacitor base on rGO gel electrode.

Although most of the nickel foam was removed, supercapacitor base on G-gel@NF-2 electrode still have good performance in high rate capability with the aid of conductive network composed of a few residual nickels as shown in Fig. 7

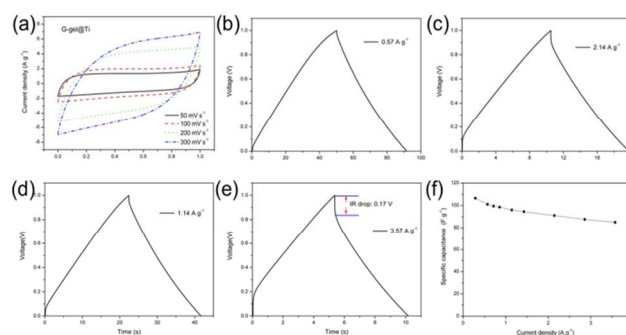


Fig. 6 (a) CV curves of G-gel@Ti at different scan rates: 50, 100, 200 and 300 mV/s. Galvanostatic charging-discharging curves at different current densities for G-gel@Ti: (b) 0.57 A g^{-1} , (c) 1.14 A g^{-1} , (d) 2.14 A g^{-1} , (e) 3.57 A g^{-1} . (f) Gravimetric specific capacitance of G-gel@Ti at different current densities

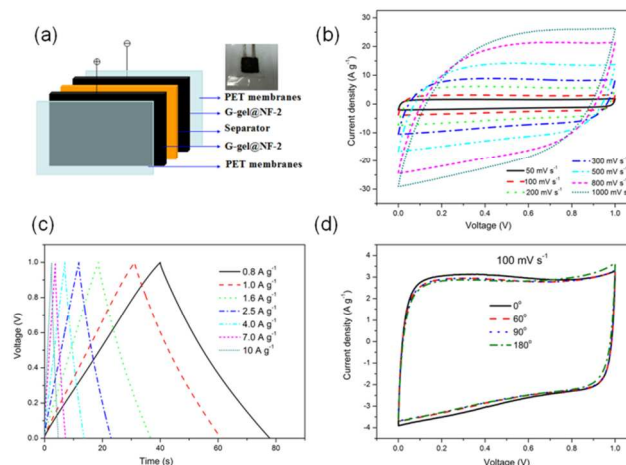


Fig. 7 (a) Schematic of the structure of flexible supercapacitors consisting of two symmetrical G-gel@NF-2 electrodes, a separator, and two PET membranes, and the digital photographs of the flexible supercapacitor. (b) CV curves of G-gel@NF-2 supercapacitor at different scan rates. (c) Galvanostatic charging-discharging curves of G-gel@NF-2 supercapacitor at different current densities. (d) The CVs of the flexible supercapacitor with bending angles of 0° , 60° , 90° and 180° at a scan rate of 100 mV s^{-1} .

Fig. 7a shows a flexible supercapacitor device assembled by two G-gel@NF-2 electrodes attached PET membranes and separator in order to better evaluate the actual performance of G-gel@NF-2. The CV curves and GCD curves of flexible supercapacitor device at different scan rates and different current densities were shown

in Fig. 7b and 7c, respectively. The CV curves are close to rectangular shape and the GCD curves are nearly a symmetric triangular shape, indicating an excellent capacitive behaviour. Although the CV curve begin to deviate a little from the quasi-rectangular shape when the scan rate was increased to 1000 mV s^{-1} because contact resistance between rGO-gel and nickel foam increases compared with G-gel @NF-1 due to mass reduction of nickel. The high specific capacitance of G-gel@NF-2 was calculated to be ~ 126 , ~ 124 and $\sim 120 \text{ F g}^{-1}$ at 0.8, 1 and 1.6 A g^{-1} according to the discharge curve (Fig. 7c), respectively. Therefore, these results suggest that most weight reduction of the nickel foam has little influence on the capacitive performance of G-gel@NF-2. Furthermore the G-gel@NF-2 supercapacitor device exhibit highly flexible and excellent mechanical robustness in the bending test. The CV curves obtained at the 100 mV s^{-1} of scan rate with various bending angle are shown in Fig. 7d. There is no significant difference between the CV curves with and without bending, suggesting the high flexible property for the G-gel@NF-2 electrode. It is very meaningful for supercapacitors in the practical application.

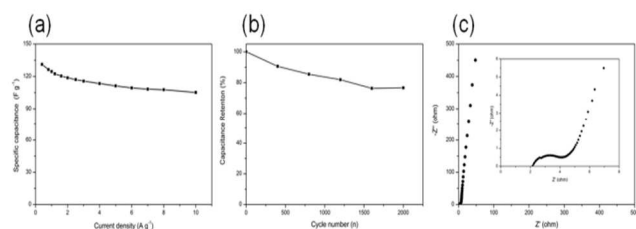


Fig.8 (a) Gravimetric specific capacitance of G-gel@NF-2 supercapacitor at different current densities. (b) Cycle stability tests for G-gel@NF-2 supercapacitor device at a current density of 4 A g^{-1} . (c) Nyquist plots of G-Gel@NF-2 supercapacitor and Inset: the high-frequency region of the plots

The gravimetric specific capacitance values at different current densities are shown in Fig. 8a. The G-gel@NF-2 maintains its $\sim 80\%$ specific capacitances with a value up to 105 F g^{-1} as the current density is increased from 0.40 to 10 A g^{-1} . The cycle stability of d G-gel@NF-2 supercapacitor shown in Fig. 8b was evaluated by repeating the GCD test at a current density of 4 A g^{-1} . The capacitance retention of G-gel@NF-2 reaches $\sim 77\%$ after 2000 cycles. These results indicate G-gel@NF-2 have a good capacitive performance. It is also confirmed by the Nyquist plots based on a frequency response analysis of frequencies ranging from 0.01 Hz to 100 kHz (Fig. 8c). At low frequencies, the straight line is nearly perpendicular to the real axis, show excellent capacitive behaviour. The equivalent series resistance (ESR) obtained from the first intersection of the semicircle with the real axis is 2.1 Ω for G-gel@NF-2, higher than that of G-gel@NF-1 because of reduction of nickel in the electrode. These results revealed that it can improve performance of rGO with the aid of conductive network composed by a few nickels. This strategy can integrate graphene into the current collector as a whole electrode, greatly reduce the total mass of the electrode, and more important is to lower the fabrication cost of supercapacitor.

Conclusions

In summary, we report a 3D graphene gel was made by a facile

simple, very efficient and industrially scalable approach. The G-gel@NF-1 supercapacitor based 3D graphene gel coated on a porous nickel framework exhibited electrochemical performance including high rate capability which the CV curves also keep ideal quasi-rectangular shape even at a high scan rate of 2000 mV s^{-1} , a high specific capacitance of $\sim 152 \text{ F g}^{-1}$ at current densities of 0.36 A g^{-1} , and good electrochemical cyclic stability which the capacitance retention still reaches $\sim 89\%$ after 2000 cycles. Furthermore the areal specific capacitance can be easily modulated to meet a variety of requirements in practical applications. A flexible G-Gel is obtained by etching most weight of the Ni foam but the conductive backbone of nickel network was still remained, and can be used as an electrode in a supercapacitor without the addition of a binder, which greatly reduces the total mass of the electrode. The gravimetric capacitance calculated using the total mass of the electrode after etching is much larger than the value before etching, which it provides a good idea to improve the performance of supercapacitors. Furthermore, flexible G-Gel supercapacitor device displays remarkable characteristics including high rate capability performance, low weight and excellent flexible properties which are very meaningful for supercapacitors in the practical application. The graphene gel coated on Ni foam can be further to form a composite electrode with metal oxides, metal hydroxide or conducting polymers to obtain higher specific capacitance. Therefore, this approach is a simple, yet highly versatile may provide a flexible, low weight, high-performance but cost-effective materials used in energy-storage devices.

Acknowledgements

This work was supported by the National Key Project of Fundamental Research of China (Grant No. 2012CB932304) and the Priority Academic Program Development of Jiangsu Higher Education Institutions

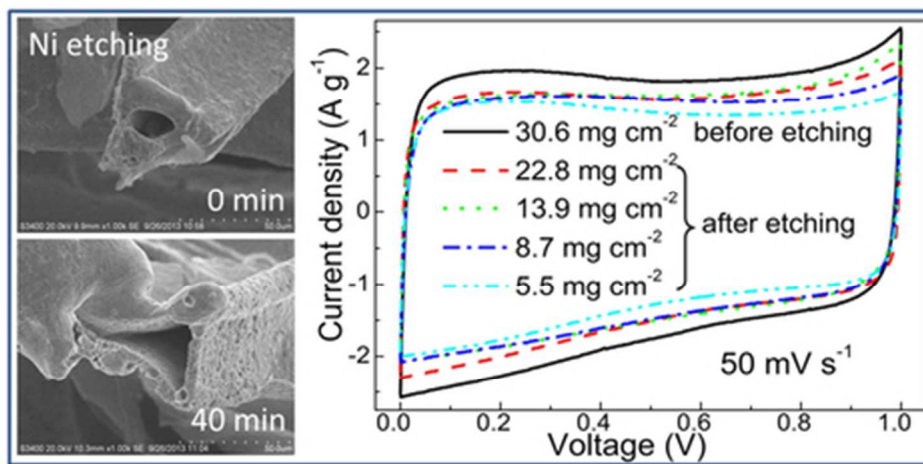
Notes and references

Nanjing National Laboratory of Microstructures, Jiangsu Provincial Laboratory for Nanotechnology and School of Physics, Nanjing University, Nanjing, 210093, P. R. China. Fax: 025-83595535; Tel: 025-83593817; E-mail: tangsl@nju.edu.cn

†Electronic Supplementary Information (ESI) available: [details of any supplementary information available should be included here]. See DOI: 10.1039/b000000x/

- J. R. Miller and P. Simon, *Science*, 2008, **321**, 651-652.
- P. Simon and Y. Gogotsi, *Nature Materials*, 2008, **7**, 845-854.
- G. Wang, L. Zhang and J. Zhang, *Chem. Soc. Rev.*, 2012, **41**, 797-828.
- T. Kuila, A. K. Mishra, P. Khanra, N. H. Kim and J. H. Lee, *Nanoscale*, 2013, **5**, 52-71
- J. R. Miller and A. F. Burke, *Electrochem. Soc. Interf.*, 2008, **17**, 53-57.
- L. L. Zhang and X. S. Zhao, *Chem. Soc. Rev.*, 2009, **38**, 2520-2531.
- A. G. Pandolfo and A. F. Hollenkamp, *J. Power Sources*, 2006, **157**, 11-27.
- D. Hulicova-Jurcakova, M. Seredych, G. Q. Lu and T. J. Bandosz, *Adv. Funct. Mater.*, 2009, **19**, 438-447.
- L. Wei, M. Sevilla, A. B. Fuertes, R. Mokaya and G. Yushin, *Adv. Funct. Mater.*, 2012, **22**, 827-834.
- E. J. Ra, E. Raymundo-Piñero, Y. H. Lee and F. Béguin, *Carbon*, 2009, **47**, 2984-2992.

11. Z. Tai, X. Yan, J. Lang and Q. Xue, *J. Power Sources*, 2012, **199**, 373-378.
12. D. N. Futaba, K. Hata, T. Yamada, T. Hiraoka, Y. Hayamizu, Y. Kakudate, O. Tanaike, H. Hatori, M. Yumura and S. Iijima, *Nat Mater*, 2006, **5**, 987-994.
13. M. Kaempgen, C. K. Chan, J. Ma, Y. Cui and G. Gruner, *Nano letters*, 2009, **9**, 1872-1876.
14. G. Lota, K. Fic and E. Frackowiak, *Energy Environ. Sci.*, 2011, **4**, 1592-1605.
15. M. D. Stoller, S. Park, Y. Zhu, J. An and R. S. Ruoff, *Nano letters*, 2008, **8**, 3498-3502.
16. Y. Huang, J. Liang and Y. Chen, *Small*, 2012, **8**, 1805-1834.
17. H. M. Jeong, J. W. Lee, W. H. Shin, Y. J. Choi, H. J. Shin, J. K. Kang and J. W. Choi, *Nano Lett*, 2011, **11**, 2472-2477.
18. C. Liu, Z. Yu, D. Neff, A. Zhamu and B. Z. Jang, *Nano Lett*, 2010, **10**, 4863-4868.
19. X. Yang, C. Cheng, Y. Wang, L. Qiu and D. Li, *Science*, 2013, **341**, 534-537.
20. C. Lee, X. Wei, J. W. Kysar and J. Hone, *Science*, 2008, **321**, 385-388.
21. S. Stankovich, D. A. Dikin, R. D. Piner, K. A. Kohlhaas, A. Kleinhammes, Y. Jia, Y. Wu, S. T. Nguyen and R. S. Ruoff, *Carbon*, 2007, **45**, 1558-1565.
22. M. Beidaghi and C. Wang, *Adv. Funct. Mater.*, 2012, **22**, 4501-4510.
23. C. Li and G. Shi, *Nanoscale*, 2012, **4**, 5549-5563.
24. J. Chen, K. Sheng, P. Luo, C. Li and G. Shi, *Adv Mater*, 2012, **24**, 4569-4573.
25. Y. Xu, Z. Lin, X. Huang, Y. Liu, Y. Huang and X. Duan, *ACS nano*, 2013, **7**, 4042-4049.
26. Y. Li, Z. Li and P. K. Shen, *Adv Mater*, 2013, **25**, 2474-2480.
27. B. G. Choi, M. Yang, W. H. Hong, J. W. Choi and Y. S. Huh, *ACS nano*, 2012, **6**, 4020-4028.
28. Z. Chen, W. Ren, L. Gao, B. Liu, S. Pei and H.-M. Cheng, *Nature materials*, 2011, **10**, 424-428.
29. H. Ji, L. Zhang, M. T. Pettes, H. Li, S. Chen, L. Shi, R. Piner and R. S. Ruoff, *Nano Lett*, 2012, **12**, 2446-2451.
30. O. C. Compton, Z. An, K. W. Putz, B. J. Hong, B. G. Hauser, L. Catherine Brinson and S. T. Nguyen, *Carbon*, 2012, **50**, 3399-3406.
31. E. Bekyarova, S. Sarkar, F. Wang, M. E. Itkis, I. Kalinina, X. Tian and R. C. Haddon, *Acc. Chem. Res.*, 2012, **46**, 65-76.
32. Y. Gogotsi and P. Simon, *Science*, 2011, **334**, 917-918.
33. B. Conway, *Electrochemical supercapacitors: scientific fundamentals and technological applications (POD)*, Kluwer Academic/Plenum: New York, 1999.
34. V. T. Le, H. Kim, A. Ghosh, J. Kim, J. Chang, Q. A. Vu, D. T. Pham, J.-H. Lee, S.-W. Kim and Y. H. Lee, *ACS nano*, 2013, **7**, 5940-5947.
35. Y. J. Kang, S.-J. Chun, S.-S. Lee, B.-Y. Kim, J. H. Kim, H. Chung, S.-Y. Lee and W. Kim, *ACS nano*, 2012, **6**, 6400-6406.
36. P. Li, C. Kong, Y. Shang, E. Shi, Y. Yu, W. Qian, F. Wei, J. Wei, K. Wang, H. Zhu, A. Cao and D. Wu, *Nanoscale*, 2013, **5**, 8472-8479.
37. L. L. Zhang, X. Zhao, M. D. Stoller, Y. Zhu, H. Ji, S. Murali, Y. Wu, S. Perales, B. Clevenger and R. S. Ruoff, *Nano Lett*, 2012, **12**, 1806-1812.
38. Z. Niu, J. Chen, H. H. Hng, J. Ma and X. Chen, *Adv Mater*, 2012, **24**, 4144-4150.
39. L. Zhang and G. Shi, *J. Phys. Chem. C*, 2011, **115**, 17206-17212.
40. M. F. El-Kady, V. Strong, S. Dubin and R. B. Kaner, *Science*, 2012, **335**, 1326-1330.
41. C. Niu, E. K. Sichel, R. Hoch, D. Moy and H. Tennent, *Applied Physics Letters*, 1997, **70**, 1480-1482.
42. C. Portet, M. A. Lillo-Rodenas, A. Linares-Solano and Y. Gogotsi, *Phys. Chem. Chem. Phys.*, 2009, **11**, 4943-4945.



A Ni network supported 3D graphene electrode was synthesized by nickel etching process, exhibited high rate capability for supercapacitor.
39x19mm (300 x 300 DPI)